Tracking electromechanical muscle dynamics using ultrafast ultrasound and high-density EMG

Waasdorp, R.; Mugge, W.; Vos, H. J.; de Groot, J.H.; De Jong, N.; Verweij, M. D.; Schouten, A. C.; Daeichin, V.

DOI
10.1109/ULTSYM.2019.8925557

Publication date
2019

Document Version
Final published version

Published in
Proceedings 2019 IEEE International Ultrasonics Symposium, IUS 2019

2019 IEEE International Ultrasonics Symposium (IUS)
Glasgow, Scotland, October 6-9, 2019

Tracking electromechanical muscle dynamics using ultrafast ultrasound and high-density EMG

R Waasdorp[a,b], W Mugge[b], HJ Vos[a,c], JH de Groot[d], N de Jong[a,c], MD Verweij[a,c], AC Schouten[b,e], V Daeichin[a,*]

***Abstract*—Current methods to track the progression and evaluate treatment of muscular dystrophies are scarce. The electromechanical delay (EMD), defined as the time lag from muscle electrical activity to motion onset, has been proposed as a biomarker, but provides only limited insight in the pathophysiology of muscle function. This work proposes and evaluates a novel method to track the propagation of electromechanical waves in muscles, using high density electromyography and ultrafast ultrasound imaging. Muscle contractions in three healthy subjects were evoked by electrical stimulation, and the subsequent propagating action potentials were successfully tracked in all 90 trials. Contractile waves were detected in 83 recordings. Detection rate varied across muscle depth. Mean (SD) velocities for the action potential were 3.71 (0.08) m/s, 4.73 (0.35) m/s and 3.27 (0.09) m/s for participant 1, 2 and 3 respectively. Velocities for the contractile wave were 3.83 (1.07) m/s, 3.32 (0.78) m/s and 3.41 (0.69) m/s for participant 1, 2 and 3 respectively. In conclusion, our technique can track the fast muscular electromechanical dynamics with high spatiotemporal resolution by combining ultrafast ultrasound imaging and high-density electromyography.**

***Index Terms*—Muscle, ultrafast ultrasound, high-density electromyography, excitation-contraction coupling, stimulation**

I. Introduction

Muscular dystrophies (MDs) are characterized by progressive muscle degeneration, resulting in weakness and decline in physical function. Ultimately, respiratory and cardiac failure can lead to death. The pathophysiology of MDs is poorly understood, and current methods to monitor the progression of the disease and evaluate the efficacy of new treatment options are limited. Assessment of maximum muscle force normalized to remaining muscle contractile cross-sectional area using quantitative muscle MRI in MD patients indicates that fiber loss cannot be the only cause for muscle weakness [1]. Likely, the force-generating capacity of the remaining muscle fibers is decreased. The change in fiber properties is possibly caused by alteration in the force transmission within the muscle fiber. This has only been demonstrated in a MD mice model [2].

[a]*Acoustical Wavefield Imaging, ImPhys, Delft University of Technology, the Netherlands*
[b]*Laboratory for Neuromuscular Control, Department of Biomechanical Engineering, Mechanical Engineering, Delft University of Technology, the Netherlands*
[c]*Biomedical Engineering, Thorax Center, Erasmus MC, Rotterdam, the Netherlands*
[d]*Department of Rehabilitation Medicine, Leiden University Medical Center, the Netherlands*
[e]*Laboratory of Biomechanical Engineering, Institute for Biomedical Technology (BMTI), University of Twente, the Netherlands*
[*]Corresponding author, E-mail address: V.Daeichin@tudelft.nl

Currently, no *in vivo* (non-invasive) experimental methods exist to determine force transmission in muscles, and thus other methods such as assessing electromechanical delay (EMD) have been proposed as an alternative biomarker. EMD is defined as the time lag between onset of muscle electrical activity and force production. Multiple studies have been conducted to assess the EMD in healthy participants using ultrafast ultrasound imaging (UUI), but the insights in alteration of muscle function are limited. Tissue motion is often averaged over a large field of view (FOV) [3], [4], which hampers accurate assessment of the local excitation-contraction (E-C) coupling in muscle fibers. The E-C is defined as the contractile response of fiber segments when excited by a propagating action potential (AP) [5].

The current study proposes a novel method to measure the local E-C, by tracking propagating electrical waves (i.e. action potentials, AP) and the subsequent contractile waves (ConW) using high density surface electromyography (HD-sEMG) and UUI. In depth analysis of the E-C coupling can advance our understanding of muscular behavior, muscle force transmission, and ultimately the pathophysiology of MD, potentially leading to a novel biomarker to track the progression of MDs and evaluate the efficacy of new treatment options [4], [5].

II. Materials and Methods

Three healthy male subjects (22-25 years) participated in the experiment. The subjects gave informed consent. The experiment was approved by the TU-Delft ethics committee.

A. Instrumentation

1) Surface EMG activity: To track the action potentials, an 8×8 square high-density (HD) electrode grid (interelectrode distance $4\,\mathrm{mm}$) was placed proximal with respect to the innervation zone (IZ) over the belly of the Biceps Brachii (BB; Figure 1). A reference Ag-AgCl electrode was placed on the wrist. Unipolar signals were sampled at $2{,}048\,\mathrm{Hz}$ using a 136-channel Refa amplifier (TMSi, Oldenzaal, the Netherlands).

2) Electrical stimulation: Muscle contractions of the BB were evoked by electrical stimulation. The stimulator (Micromed Energy, Micromed S.p.A., Mogliano Veneto, Italy) gave a single pulse with only negative phase, with a pulse duration of $200\,\mu\mathrm{s}$ and an amplitude between 5-10 mA. The cathode was placed over the innervation zone of the BB.

978-1-7281-4596-9/19/$31.00 ©2019 IEEE

3) Ultrasonography: Muscle contractions were imaged using linear transducer array (L12-5 $50\,\mathrm{mm}$ 256 element probe; Philips, Bothell, WA, USA) connected to a Vantage-256 research ultrasound scanner (Verasonics Inc., Kirkland, WA, USA). The scanner was set to transmit plane waves with a center frequency of $7.8\,\mathrm{MHz}$, and sampled the raw radio frequency (RF) signals at 4 times the center frequency. Since the scanner consists of 128 channels per transducer connector, one image was formed with three synthetic aperture transmit and receive events. Imaging depth was set to $16\,\mathrm{mm}$, resulting in an effective frame rate of $5{,}000$ frames per second. Per trial $100\,\mathrm{ms}$ were recorded, corresponding to 500 frames.

4) Triggering and synchronization: To trigger the stimulator and to allow synchronization of the recordings of the ultrasound scanner and EMG amplifier in data processing, a transistor-transistor logic (TTL) pulse was send from the ultrasound scanner to an arbitrary waveform generator (AWG; DG1022A, Rigol, Beijing, China) at the start of each ultrasound acquisition. The AWG send a TTL signal to the inputs of the EMG amplifier and stimulator with a delay of $20.00\,\mathrm{ms}$, to have sufficient baseline without motion.

B. Protocol

Participants were seated in a comfortable height-adjustable chair, and were asked to rest their arm on the table. First, the motor point was detected by placing the stimulator on the distal portion of the BB, around ⅔ of the length of the BB. The stimulator was moved around over the BB while repeatedly stimulating, until a point with most intense contraction was found (determined visually). Once found, the stimulator was fixated using an elastic arm strap. Before placement of the EMG electrodes, the skin on the upper arm and wrist was shaved if necessary and cleaned with an abrasive skin preparation gel and alcohol to reduce skin impedance. Next, the ultrasound transducer was placed on top the HD-EMG electrodes, and fixated using a 6 degree-of-freedom mechanical magnetic measuring stand with central locking mechanism. The transducer position was adjusted until the edges of the HD-EMG grid were visible on both sides, and the majority of the muscle fibers in the FOV were aligned with the lateral axis (verified by low frame rate real-time imaging).

The experiment consisted of three sets of ten electrical stimulations, with an inter-stimulus interval of $5\,\mathrm{s}$ and a 5 minute break between sets. After the break, the stimulator position was checked to still elicit a contraction and adjusted if needed.

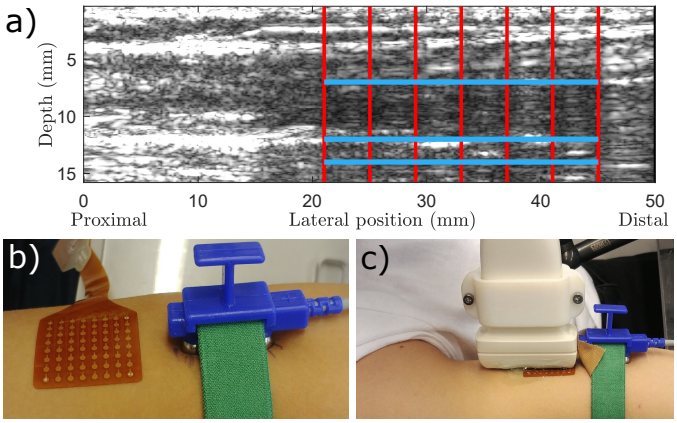

Fig. 1. **(a)** Ultrasound image of the Biceps Brachii (BB), red lines represent the location of the bipolar center of the EMG signals, blue lines show the three M-modes for different depths. The acoustic shadow caused by the EMG grid is visible on the right side of the image. **(b)** Stimulator positioned on the innervation zone (IZ) of the BB, HD-EMG electrodes positioned distal with respect to the IZ. **(c)** ultrasound transducer placed on top of the HD-EMG electrodes.

C. Processing

Ultrasound and EMG signals were processed in Matlab R2018b (The MathWorks, Natick, MA, USA).

1) EMG velocity estimation: EMG signals were first spatially filtered using the longitudinal single differential (along fiber direction) to obtain bipolar signals [6]. Next, the signal was band-pass filtered using a bidirectional 3rd order Butterworth filter (cutoff frequencies 10-250Hz). Trials with low amplitude EMG signal ($< 500\,\mu\mathrm{V}$) were excluded from the analysis. To find the velocity of the action potential propagating through the muscle, a parametric model was fit to the measured data. The bipolar EMG signals elicited by electrical stimulation were found to have a negative and a positive peak with different amplitude and length. Therefore, two sines with sufficient parameters to resemble the shape of the EMG signals were chosen as the basis for the signal model. The measured bipolar signal per electrode over time is given by $y_{ij}^{m}(t)$, with $i = 1...N$ the electrode row (proximal to distal) and $j = 1...M$ the electrode column (medial to lateral). For the used 8×8 electrode grid, $N = 7$ and $M = 8$, corresponding to the 56 bipolar channels. The signal model is given by,

$$\begin{aligned} y_{ij}^{s}(t) = {} & w_{1ij}(t)\sin\left(\tfrac{2\pi}{T_1}\left(t-\tau_{ij}\right)\right) - \\ & w_{2ij}(t)\sin\left(\tfrac{2\pi}{T_2}\left(t-\tfrac{T_1}{2}-\tau_{ij}\right)\right), \end{aligned} \tag{1}$$

with window functions,

$$w_{1ij}(t) = \begin{cases} A_1, & \tau_{ij} < t \le \tau_{ij} + \frac{T_1}{2} \\ 0, & \text{otherwise,} \end{cases} \tag{2a}$$

$$w_{2ij}(t) = \begin{cases} A_2, & \tau_{ij} + \frac{T_1}{2} < t \le \tau_{ij} + \frac{T_1+T_2}{2} \\ 0, & \text{otherwise.} \end{cases} \tag{2b}$$

The windows with different amplitudes and lengths allowed fitting on the asymmetric shaped action potentials. The delay τ_{ij} is given by,

$$\tau_{ij} = \tau_{\text{arr}} - \tau_{\text{x}ij} - \tau_{\text{y}ij}, \tag{3}$$

and depends on a common delay τ_{arr} depending on the distance of a reference electrode to the IZ, and a delay depending on the location of each individual electrode,

$$\tau_{\text{x}ij} = (i-1)\tfrac{d_{\text{ie}}}{V_{\text{AP}}}, \qquad \tau_{\text{y}ij} = (j-1)\tfrac{d_{\text{ie}}\tan(\theta)}{V_{\text{AP}}}, \tag{4}$$

where d_{ie} denotes the interelectrode distance, V_{ap} the velocity of the action potential, and θ the angle of the propagating

wave to accommodate for the skewness of end-plate positions on the muscle fibers [7].

For each participant and trial, the model was fit to normalized bipolar EMG data, i.e. $\bar{y}^m_{ij}(t) = y^m_{ij}(t)/\sigma_{ij}$, with σ_{ij} the standard deviation of channel ij. Channels with a root mean square (RMS) lower than $10\,\%$ of mean RMS of all channels were excluded from the fitting procedure. The fitting criterion was defined by,

$$E = \sum_{i=1}^{N} \sum_{j=1}^{M} \|\bar{y}^m_{ij}(t) - y^s_{ij}(t)\|^2. \tag{5}$$

The validity of the found parameters after convergence was assessed by the variance accounted for (VAF), which was determined per channel,

$$\mathrm{VAF}_{ij} = \left[1 - \frac{\sum_{n_{ij}}^{m_{ij}} (\bar{y}^m_{ij}(t) - y^s_{ij}(t))^2}{\sum_{n_{ij}}^{m_{ij}} (\bar{y}^m_{ij}(t))^2}\right] \cdot 100\%, \tag{6}$$

where n_{ij} corresponds to the first and m_{ij} to the last sample within the window of channel ij, i.e. where $y^s_{ij}(t) \neq 0$. This was done to avoid influence of stimulation artifacts and complex MUAP shapes on the VAF that the model could not explain. Next the mean VAF was determined as

$$\mathrm{VAF} = \frac{1}{NM} \sum_{i=1}^{N} \sum_{j=1}^{M} \mathrm{VAF}_{ij}. \tag{7}$$

The found parameters were later used to simulate the EMG signal as a reference to find the onset of tissue motion, described below.

2) Ultrasonography: Raw RF signals were processed to In phase-Quadrature data using conventional delay and sum beamforming, resulting in $S(x, z, t_i)$. The EMG and ultrasound data were spatially aligned using the acoustic shadow present due to the electrode grid. Local tissue velocities $v_z(x, z, t_i)$ along the ultrasound beam axis (i.e. z-axis, depth) were determined using one-lag autocorrelation speckle tracking [8]. The tissue velocities v_z were temporal filtered using a 6th order Butterworth low-pass filter (cutoff frequency $100\,\mathrm{Hz}$). Next v_z was differentiated to obtain axial tissue acceleration,

$$a_z(x, z, t_i) = (v_z(x, z, t_i) - v_z(x, z, t_{i-1}))\, F_s, \tag{8}$$

with F_s the frame rate. The ConW was tracked using a normalized Radon transform of the acceleration a_z [9]. To find the onset of tissue motion, only $a_z(x, z, t_i)$ within a time window of moment of first detection of EMG activity and the second (positive) peak in the EMG was used,

$$\min_{ij}(\tau_{ij}) - 5\,\mathrm{ms} < t_i \leq \min_{ij}(\tau_{ij}) + \tfrac{T_1}{2} + \tfrac{T_2}{4}. \tag{9}$$

Furthermore, only data in a region of interest (ROI), chosen directly below the EMG grid, was used to track the ConW (parallelogram in Figure 2). Three different horizontal M-modes in the ultrasound image with good speckle from the muscle fibers were chosen for the analysis. Acceleration data along these M-modes (averaged over $\pm 0.5\,\mathrm{mm}$ in depth), within the ROI and the time of window of interest was used to track the ConW, resulting in a velocity V_{conw} and time of arrival $T_{\text{arr-conw}}$. Peaks in the Radon transform corresponding to a velocity outside $V_{\text{ap}} \pm 2\,\mathrm{m\,s^{-1}}$ were regarded as false positives and excluded.

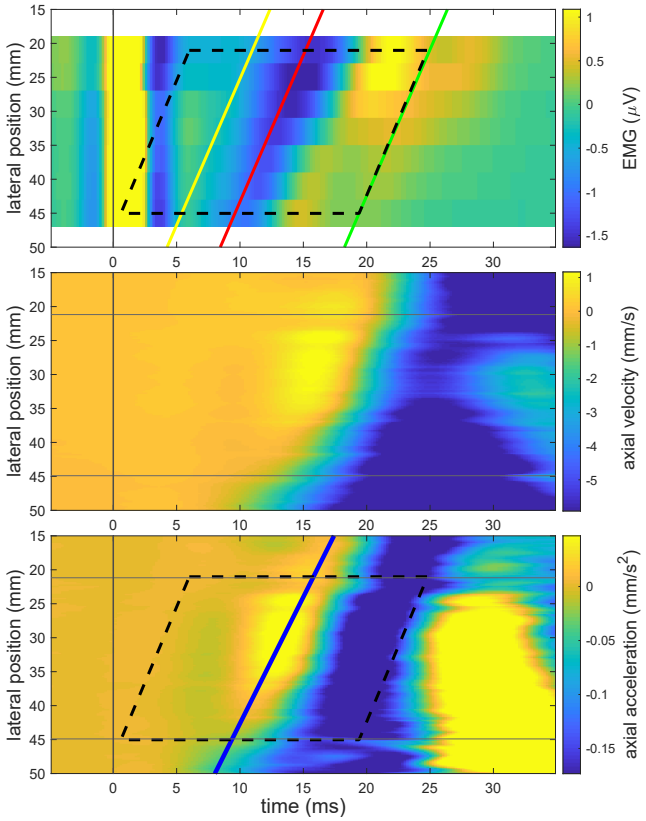

Fig. 2. Typical result for participant 2, M-mode at depth $12\,\mathrm{mm}$. **Top:** EMG of column beneath ultrasound probe. Velocity of the action potential $V_{\text{ap}} = 4.31\,\mathrm{m\,s^{-1}}$. The yellow line denotes the onset of EMG activity, the red line the depolarizing peak corresponding to $T_{\text{arr-ap}} = 9.60\,\mathrm{ms}$ and the green line the subsequent positive peak. The yellow peak at $t = 0\,\mathrm{ms}$ is a stimulation artifact. **Center:** axial tissue velocity along the M-mode. **Bottom:** axial tissue acceleration. The data within the dashed parallelogram (ROI) was Radon transformed to track the contractile wave, resulting in velocity $V_{\mathrm{conw}} = 3.72\,\mathrm{m\,s^{-1}}$ and arrival time $T_{\text{arr-conw}} = 9.38\,\mathrm{ms}$. The tracked wave is indicated by the blue line.

III. Results

The velocity of the AP was found in all trials for all participants, see Table I. The EMG measurement was highly repeatable, illustrated in Figure 3. The VAF was in 83 out of 90 trials above 70%, denoting reliable model fits. The Radon transform of the acceleration data within the ROI successfully tracked ConW in 83 trials. The tracking results varied with M-mode depth, and the total of 90 Radon transforms per participant resulted in a success rate of 57% for participant 1, 73% for participant 2 and 59% for participant 3. Both the velocity and time of arrival of the ConW had larger spread than the AP velocity and time of arrival, as can be seen by the standard deviations. In some cases, the arrival time of the ConW preceded the arrival of the AP (e.g. participant 1, M-modes 10 and $14\,\mathrm{mm}$). In Figure 2, a typical result for one trial is presented.

TABLE I

Results for three participants, M denotes mean, SD standard deviation, SR success rate. The velocity of the action potential V_{ap} was found for all trials (SR EMG fit). $T_{\text{arr-ap}}$ denotes the arrival time of the depolarizing peak in the action potential. The number of successful fits and the results for Radon transforming acceleration data to find the velocity V_{conw} of the contractile wave are presented for three M-modes at various depths. $T_{\text{arr-conw}}$ denotes the arrival time of the contractile wave.

Participant	SR EMG fit	V_{ap} (m s^{-1}) M	V_{ap} (m s^{-1}) SD	$T_{\text{arr-ap}}$ (ms) M	$T_{\text{arr-ap}}$ (ms) SD	VAF (%) M	VAF (%) SD	M-mode depth (mm)	SR Radon fit	V_{conw} (m s^{-1}) M	V_{conw} (m s^{-1}) SD	$T_{\text{arr-conw}}$ (ms) M	$T_{\text{arr-conw}}$ (ms) SD
1	30/30	3.71	0.082	6.48	1.96	81.47	3.49	5	26/30	3.48	1.30	7.20	4.77
								10	15/30	4.14	0.78	0.56	0.81
								14	20/30	4.04	0.82	1.75	2.00
2	30/30	4.73	0.349	9.38	0.81	77.58	7.85	5	20/30	2.89	0.34	11.12	1.24
								12	18/30	4.01	1.14	7.02	3.23
								14	28/30	3.18	0.27	8.84	0.83
3	30/30	3.27	0.086	10.87	0.42	77.29	2.56	5	29/30	3.34	0.38	14.97	0.72
								10	15/30	3.26	1.11	9.87	2.86
								14	9/30	3.84	0.36	10.94	0.66

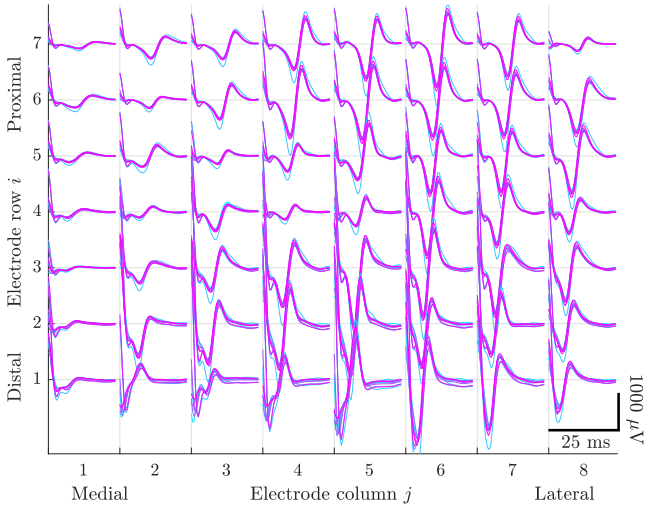

Fig. 3. Measured EMG signals of all electrodes y_{ij}^m for one set of 10 stimuli plotted on top of one another, indicating high repeatability across trials within a set. At the start of each signal, the stimulation artifact can be seen.

IV. Discussion and Conclusions

The current study demonstrated that fast electromechanical muscle dynamics can be tracked using high-density electromyography and ultrafast ultrasound imaging. Velocities of AP and ConW were within the same order of magnitude. There are several possible causes for the higher standard deviation in V_{conw}. First, the ultrasound data acquisition and analysis are more complex than the EMG recording and processing. The results are highly dependent on image quality, which varies per participant and ultrasound probe orientation with respect to the fibers. Second, the ConW tracking was very sensitive to local peaks in the Radon domain. Selection of peaks based on acceleration data within the parallelogram shaped ROI decreased the spread and improved the success rate. Third, there was spread in the time instant of the positive peak in the acceleration data across lateral positions. This was presumably caused by the interrupted speckle pattern of the muscle fiber due to acoustic shadow caused by the EMG grid.

In some trials, the detected ConW arrived earlier than the AP. This observed motion is presumably caused by contraction of earlier activated fiber segments closer to the IZ, pulling on fiber segments within the ROI. In most trials, low amplitude negative acceleration prior to the tracked ConW was observed (greenish area preceding positive acceleration in Figure 2). This indicates that, although ConWs could be detected, the physiological meaning of the detected wave's velocity and arrival time remains elusive.

In conclusion, our technique can track the fast muscular electromechanical dynamics with high spatiotemporal resolution by combining UUI and HD-EMG. The data acquisition and processing have to be further improved to detect the ConW more robustly, and to further our understanding of the ConW's relation to the underlying muscle physiology. Moreover, the influence of experimental conditions on the measured muscle motion has to be assessed, e.g. influence of stimulation intensity, arm position, distance of ROI to IZ and variation across M-mode depths.

References

[1] B. H. Wokke, J. C. van den Bergen, M. J. Versluis, E. H. Niks, J. Milles, A. G. Webb, E. W. van Zwet, A. Aartsma-Rus, J. J. Verschuuren, and H. E. Kan, "Quantitative MRI and strength measurements in the assessment of muscle quality in Duchenne muscular dystrophy," vol. 24, no. 5, pp. 409–416.

[2] D. R. Claflin and S. V. Brooks, "Direct observation of failing fibers in muscles of dystrophic mice provides mechanistic insight into muscular dystrophy," vol. 294, no. 2, pp. C651–C658.

[3] A. Nordez, T. Gallot, S. Catheline, A. Guével, C. Cornu, and F. Hug, "Electromechanical delay revisited using very high frame rate ultrasound," vol. 106, no. 6, pp. 1970–1975.

[4] L. Lacourpaille, F. Hug, A. Guével, Y. Péréon, A. Magot, J.-Y. Hogrel, and A. Nordez, "New insights on contraction efficiency in patients with Duchenne muscular dystrophy," vol. 117, no. 6, pp. 658–662.

[5] A. Sandow, "Excitation-Contraction Coupling in Muscular Response," vol. 25, no. 3, pp. 176–201.

[6] S. Dick F., K. Bert U., L. Bernd G., and V. D. Johannes P., "High-density Surface EMG: Techniques and Applications at a Motor Unit Level," vol. 32, no. 3, pp. 3–27.

[7] D. F. Stegeman, J. H. Blok, H. J. Hermens, and K. Roeleveld, "Surface EMG models: Properties and applications," vol. 10, no. 5, pp. 313–326.

[8] T. Deffieux, J. Gennisson, M. Tanter, and M. Fink, "Assessment of the mechanical properties of the musculoskeletal system using 2-D and 3-D very high frame rate ultrasound," vol. 55, no. 10, pp. 2177–2190.

[9] H. J. Vos, B. M. van Dalen, I. Heinonen, J. G. Bosch, O. Sorop, D. J. Duncker, A. F. W. van der Steen, and N. de Jong, "Cardiac Shear Wave Velocity Detection in the Porcine Heart," vol. 43, no. 4, pp. 753–764.